Chula Med J Vol. 61 No. 3 May - June 2017

Agreement of bone metastasis detection between bone scintigraphy and whole body-MRI in hepatocellular carcinoma

Wittawin Sakdapetsiri *

Numphung Numkarunarunrote** Tawatchai Chaiwatanarat**

Sakdapetsiri W, Numkarunarunrote N, Chaiwatanarat T. Agreement of bone metastasis detection between bone scintigraphy and whole body-MRI in hepatocellular carcinoma. Chula Med J 2017 May – Jun;61(3): 321 - 31

Background : *Bone scintigraphy is generally accepted as the best imaging study for early detection of bone metastases. However, bone metastases from hepatocellular carcinoma (HCC), unlike other primary tumors, are largely osteolytic in nature and may be poorly visualized by bone scintigraphy (BS). Whole-body magnetic resonance imaging (MRI) has become feasible with recent developments, including fast image acquisition. So far, there has been no report of the performance of either imaging tool in the detection of bone metastasis from HCC.*

Objective : *To study the agreement of bone metastatic detection by bone scintigraphy and whole-body MRI in hepatocellular carcinoma patients.*

Methods : *A prospective study was carried out in 16 patients with HCC (mean age 54 years, range 41 - 70 years). All patients were assessed for bone metastasis with bone scintigraphy using Tc-99m methylene diphosphonate (MDP) and whole-body MRI (coronal whole body and sagittal spine T1 weighted and short tau inversion recovery sequences). The bone lesions were assessed on each imaging investigation independently. Each patient was categorized into 1 of 4 categories, i.e. positive, probably positive, probably negative and negative. Extra-osseous metastases on MRI were also recorded.*

* Synphaet Hospital, Bangkok, Thailand.

** Department of Radiology, Faculty of Medicine, Chulalongkorn University

Results : *The study showed moderate agreement of bone metastasis detection between bone scintigraphy and whole body-MRI in patients with HCC (kappa = 0.5 with 95% CI = 0.19 - 0.81). Eight of the 16 patients (50%) were concordantly categorized. Whole body-MRI tended to identify more positive lesions in the spine, pelvis and appendicular skeleton, whereas bone scintigraphy tended to show more positive lesions in the ribs. Whole body-MRI identified extra-osseous metastases in 9 patients (56%), these included the lung, pelvic cavity and intramuscular of the thigh.*

Conclusions : *There is moderate agreement of bone metastasis detection between bone scintigraphy and whole body-MRI in patients with HCC. MRI tends to detect more lesions and is also useful for extra-osseous metastasis.*

Keywords : *Bone metastasis, bone scintigraphy, whole body-MRI, hepatocellular carcinoma.*

Correspondence to: Chaiwatanarat T. Department of Radiology, Faculty of Medicine, Chulalongkorn University, Bangkok 10330, Thailand.

Received for publication. November 2, 2016.

วิธวินท์ ศักดาเพชรศิริ, น้ำผึ้ง นำการุณอรุณโรจน์, ธวัชชัย ชัยวัฒนรัตน์. ความสอดคล้องกันของการตรวจการแพร่กระจายมะเร็งตับไปยังกระดูกด้วยการตรวจสแกนกระดูกและการตรวจด้วยคลื่นแม่เหล็กไฟฟ้าแบบทั้งตัว. จุฬาลงกรณ์เวชสาร 2560 พ.ค. – มิ.ย.;61(3): 321 – 31

เหตุผลของการทำวิจัย : *เป็นที่ยอมรับกันโดยทั่วไปว่าการตรวจสแกนกระดูกเป็นการตรวจด้วยภาพที่ดีที่สุดในการตรวจการแพร่กระจายของมะเร็งไปยังกระดูก อย่างไรก็ดีการแพร่กระจายของมะเร็งตับมาที่กระดูกมักมีลักษณะเป็น osteolytic เท่านั้น ซึ่งต่างจากมะเร็งอื่น ๆ หลายชนิด ทำให้อาจจะไม่สามารถตรวจพบได้ด้วยการตรวจสแกนกระดูก ในปัจจุบันการตรวจด้วยคลื่นแม่เหล็กไฟฟ้า (MRI) แบบทั้งตัวสามารถทำได้เร็วขึ้น ยังไม่มีรายงานการศึกษาประสิทธิภาพการตรวจพบการแพร่กระจายมะเร็งตับไปยังกระดูกด้วยการตรวจทั้งสองวิธี*

วัตถุประสงค์ : *เพื่อศึกษาความสอดคล้องกันของการตรวจการแพร่กระจายของมะเร็งตับไปยังกระดูกด้วยการทำสแกนกระดูกและการตรวจด้วยคลื่นแม่เหล็กไฟฟ้าแบบทั้งตัว*

วิธีการศึกษา : *การศึกษาแบบไปข้างหน้าในผู้ป่วยมะเร็งตับ 16 ราย (อายุเฉลี่ย 54 ปี อายุระหว่าง 41 - 70 ปี) ผู้ป่วยทุกรายได้รับการประเมินการแพร่กระจายไปยังกระดูกของมะเร็งด้วยการตรวจสแกนกระดูก (ด้วย Tc-99m MDP) และการตรวจด้วยคลื่นแม่เหล็ก ไฟฟ้าแบบทั้งตัว (coronal whole body and sagittal spine T1 weighted and short tau inversion recovery sequences) การประเมินรอยโรคในกระดูกด้วยการตรวจทั้ง 2 วิธี โดยแยกจากกัน ผู้ป่วยแต่ละรายถูกจัดแบ่งเป็น 1 ใน 4 กลุ่มได้แก่ ผลบวก อาจเป็นผลบวก อาจเป็นผลลบ และผลลบ การแพร่กระจาย ไปบริเวณที่ไม่ใช่กระดูกที่ตรวจพบได้ด้วย MRI และได้รับการบันทึกไว้ด้วย*

ผลการศึกษา : *ผลการศึกษาพบว่ามีความสอดคล้องกันในระดับปานกลาง สำหรับการตรวจการแพร่กระจายไปยังกระดูกของมะเร็งตับระหว่างการตรวจสแกนกระดูกและการตรวจด้วยคลื่นแม่เหล็กไฟฟ้าแบบทั้งตัว (kappa = 0.5 ด้วย 95% CI = 0.19 - 0.81) ผู้ป่วย 8 ใน 16 ราย (ร้อยละ 50) มีผลการตรวจทั้ง 2 วิธีตรงกัน การตรวจด้วยคลื่นแม่เหล็กไฟฟ้าแบบทั้งตัวมีแนวโน้มที่จะสามารถตรวจพบรอยโรคได้มากกว่าในบริเวณกระดูกสันหลัง กระดูกเชิงกรานและกระดูกแขนขา ในขณะที่การตรวจสแกนกระดูกมีแนวโน้มที่จะสามารถตรวจพบรอยโรคได้มากกว่าในบริเวณกระดูกซี่โครง การตรวจด้วยคลื่นแม่เหล็กไฟฟ้าแบบทั้งตัวสามารถตรวจพบมะเร็งแพร่กระจายในบริเวณที่ไม่ใช่กระดูกในผู้ป่วย 9 ราย (ร้อยละ 56) ได้แก่ ปอด ช่องเชิงกราน และในกล้ามเนื้อต้นขา*

สรุป : *การตรวจการแพร่กระจายไปยังกระดูกของมะเร็งตับระหว่างการตรวจสแกนกระดูกและการตรวจด้วยคลื่นแม่เหล็กไฟฟ้าแบบทั้งตัวมีความสอดคล้องกันในระดับปานกลาง การตรวจด้วยคลื่นแม่เหล็กไฟฟ้าแบบทั้งตัวมีแนวโน้มที่จะสามารถตรวจพบรอยโรคได้มากกว่า และรวมถึงรอยโรคมะเร็งแพร่กระจายในบริเวณที่ไม่ใช่กระดูกด้วย*

คำสำคัญ : *มะเร็งแพร่กระจายไปยังกระดูก, การตรวจสแกนกระดูก, การตรวจด้วยคลื่นแม่เหล็กไฟฟ้าแบบทั้งตัว, มะเร็งตับ.*

Hepatocellular carcinoma (HCC) is the most common primary hepatic malignancy in adults, particularly in certain regions of Asia. [1] The prognosis has been improved by modern imaging techniques allowing an early diagnosis and by the value of the therapeutic protocols employed Staging has also become increasingly important.[1]

The lung, abdominal lymph nodes and bones are the most common sites of extrahepatic metastatic HCC; they mostly occur in those with advanced intrahepatic tumor stage (stage IVA).[2] The plain film appearance of skeletal metastases from HCC was osteolytic in all cases. [1] Computed tomography (CT) scan is the best tool for demonstrating the destructive nature of these metastases which are often associated with large, bulky soft-tissue masses.[1] The most frequent sites of skeletal metastases of HCC are the ribs, spine, femur, pelvis, and humerus. [1] Many centers consider bone scintigraphy (BS) the best imaging technology for early detection of bone metastases.[5] These metastases are usually depicted on BS when sufficient osteoblastic reaction has occurred. [3] However, bone metastases from HCC, unlike other primary tumors, are largely osteolytic in nature. [1] Hence, they elicit a particularly poor osteoblastic response and may be poorly visualized by BS.

Whole-body magnetic resonance imaging (WB-MRI) has become feasible with recent developments, including fast image acquisition, hardware innovation, and dedicated software. [4] This imaging modality has been shown to be of greater sensitivity and comparable specificity compared to BS in the detection of skeletal metastases. [4 - 6] Most studies have investigated groups of patients with a variety of tumor types, with breast, prostate and lung being the most frequently studied. There has been, however, no report of the performance of either imaging tool in the detection of bone metastasis from HCC. Our purpose is, therefore, to study the agreement of bone metastasis detection between BS and WB-MRI in patients with HCC.

Materials and Methods

Patients

This study was a prospective study. Patients diagnosed with HCC underwent BS and WB-MRI within an interval of one month. The inclusion criterion was HCC patient with suspected bone metastases by clinical or imaging studies. Exclusion criteria were: 1) known bone metastasis; 2) contraindication for BS, such as pregnancy and breast feeding; and 3) contraindication for MRI, such as claustrophobia or wearing a pacemaker. The study has been approved by the Institutional Review Board (IRB) and all subjects recruited have signed their written informed consent forms.

Imaging techniques

Bone scintigraphy

Whole-body BS was performed after intravenous administration of 740 MBq. (20 mCi.) of technetium-99m methylene diphosphonate (Tc-99m MDP). Delayed images at approximately three hours after injection were obtained as follows: anterior and posterior whole-body, right and left lateral skull, four oblique views of chest, and anterior and posterior pelvis. Other additional views were obtained if lesion clarification was needed.

Whole-body MRI

WB-MRI was performed using a 1.5 Tesla system (Ingenia, Philips) and 3 Tesla system (Archieva, Philips). All images were acquired with multicoils for 1.5 Tesla and Q-body Coil for 3 Tesla. T1-weighted (TR 412 ms & TE 4 ms for 1.5 T and TR 652 ms & TE 10 ms for 3 T) and short-tau inversion-recovery (STIR) (TR 680.3 ms & TE 66 ms for 1.5 T and TR 8412.98 ms & TE 62.75 ms for 3 T) images were acquired for six different body stations from head to toe. Sagittal images of the spine were also acquired using TSE T1 -weighted (TR 554.47 ms & TE 16 ms for 1.5 T and TR 543 ms & TE 10 ms for 3 T), T2-STIR sequences (TR 2500 ms & TE 70 ms for 1.5 T and TR 3500 ms & TE 70 ms for 3 T). At each station, 35 slices were acquired using breath-hold scans for the thorax and abdomen. Intravenous paramagnetic contrast agent was not administered. Overall scan time was approximately 60 min, including positioning and survey acquisitions. Both the T1 weighted and the STIR images at each station were reconstructed to form the whole-body image.

Imaging interpretation

BS was interpreted by an experienced nuclear medicine physician. WB-MRI study was interpreted by a radiologist with expertise in musculoskeletal MRI. The reading radiologists were unaware of patients' clinical and other imaging results. Each lesion was categorized into one of four categories, i.e. positive, probably positive, probably negative and negative. Positive indicates malignant lesion and negative is for benign lesions or no lesion detected. It was not possible to set criteria for categorization on BS, so the characteristics of the lesion, e.g. number, site, extension, intensity, etc., were taken into consideration and interpretation was based on the experience of a nuclear medicine physician. On WB-MRI, a skeletal lesion of intermediate to high signal intensity on STIR image and low signal intensity (SI) on T1 weighted image was considered positive. For the spine, a positive lesion included bulging of the posterior margin of a vertebral body, signal intensity change extending to pedicles and para-osseous tumor extension. A lesion that was located adjacent to a degenerative change of the vertebral endplates or near a joint surface, or when the lesion showed high SI on T1WI or low SI on T2WI, was considered benign. Each patient was catogorized into one of the four categories according to the highest category of lesion presented.

Statistical analysis

Using PASS 11 software with Power = 0.90 and K1 = 0.8, the estimated sample size for *Kappa* statistics was 21 lesions. Linear weighted *Kappa* statistics were calculated to determine agreements in detection of skeletal metastases between BS and WB-MRI based on per-patient.

Results

Characteristics of the patients and their lesions are shown in Table 1. A total of 16 patients, 14 males and two females with average age of 54.5 year-old, were recruited into the study. Eight patients were stage IIIB and eight were stage IVB with lung metastasis. There were a total of 62 lesions detected by both modalities. Patients' categorizations by the two modalities are shown in Table 2. Eight of the 16 patients (50%) were concordantly categorized. Six and seven patients were positively (positive or probably

positive) classified by WB-MRI and BS, respectively; four of these were concordantly categorized. Ten and nine patients were negatively (negative or probably negative) classified by WB-MRI and BS, respectively; four of these were concordantly categorized. The two modalities categorized three of 16 patients (19%) into the opposite direction, i.e. two patients as positive or probably positive by BS were negative by MRI and one vice versa. Calculated per-patient weighted *kappa* agreement was 0.5 (95% CI = 0.019 - 0.81).

Anatomical locations of lesions are shown in Table 1. Of the 20 lesions that were negatively classified on BS but positively classified on WB-MRI, 11 were in the pelvis (65% of all pelvic lesions), six in the spine (46% of all spine lesions) (Figure 1) and three were appendicular (19% of all appendicular lesions). Of the seven lesions that were probably positive by BS but negative by WB-MRI, five were in the rib (Figure 2) and two in the spine.

Additionally, an extra-osseous lesion was identified in nine patients (56%) on WB-MRI (Figure 3); it could not be demonstrated on BS. The sites of extra-osseous lesions were lung (n = 8), pelvic cavity (n =1) and intramuscular in buttock and thigh (n = 1).

Table 1. Characteristics of patients (n = 16) and lesions (n = 62).

Gender	Number (patients)
Male	14
Female	2
Mean Age (range)	54.5 (41 - 70) years
Staging	**Number (patients)**
Stage IIIB	8
Stage IVB lung metastasis	8
Site of lesion detected by both modalities	**Number (lesions)**
Pelvis	17
Appendicular	16
Spine	13
Rib	11
Others (scapula, maxilla, mandible, frontal bone and sternum)	5

Table 2. Patients' categorization by the two modalities (n = 16).

		Bone scan				
		Positive	**Probably positive**	**Probably negative**	**Negative**	**Total**
MRI	Positive	3	1	0	0	4
	Probably positive	0	1	0	1	2
	Probably negative	0	0	0	0	0
	Negative	0	2	4	4	10
	Total	3	4	4	5	16

The weighted kappa = 0.5 with (95% CI = 0.19 - 0.81)

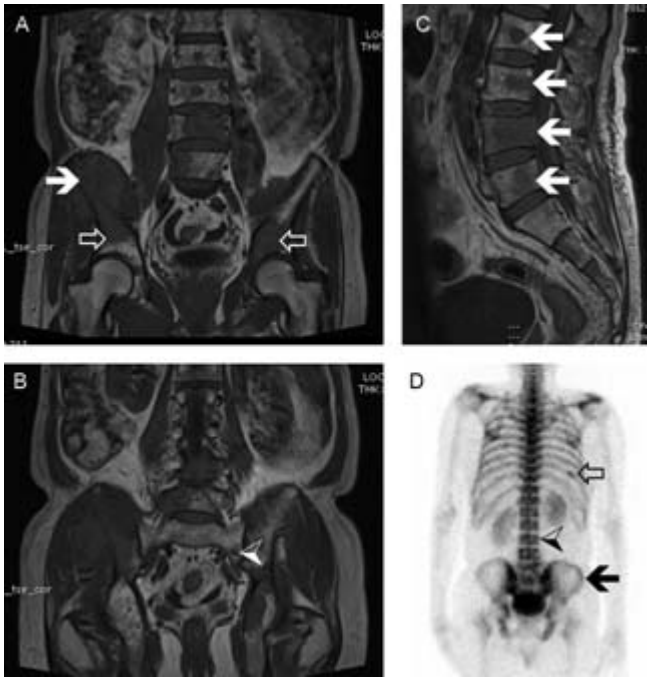

Figure 1. (A,B) Coronal T1 weighted images show positive lesions at right iliac bone (white arrow), bilateral acetabuli (open arrow) and left sacral ala (arrow head). (C) Sagittal spone T1 weighted image shows positive lesions at L2 – L5 vertebral bodies (white arrows). (D) Bone scintigraphy shows faintly increased tracer uptake, probably positive lesion at right iliac bone (black arrow) and a probably negative lesion at posterior right 9th rib (open arrow), while lumbar spine appears to have slightly decreased tracer uptake (arrow head) and is interpreted as negative.

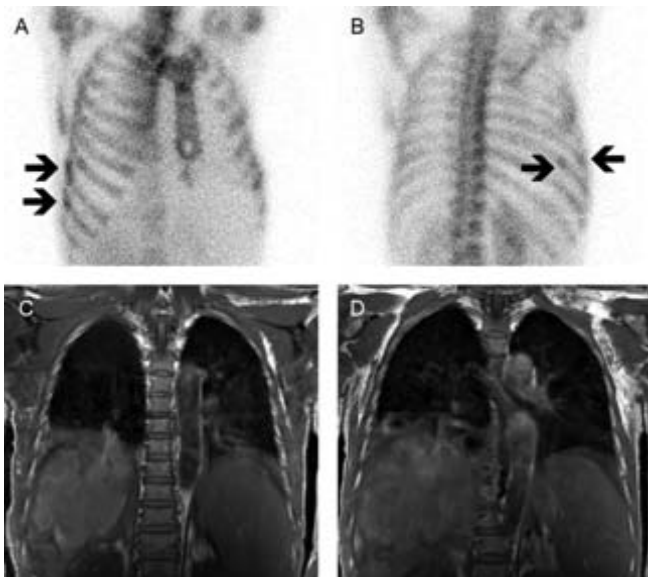

Figure 2. (A, B) Bone scintigraphy shows probably positive lesions at lateral right 7 – 8 ribs (arrow) but no lesion can be detected on coronal T1 weighted image (C,D).

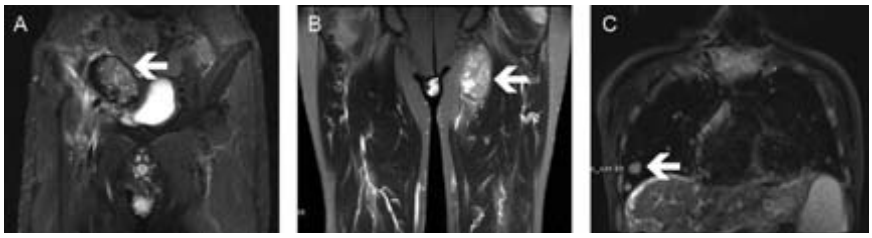

Figure 3. Extra-osseous soft-tissue matastases: (A) Coronal short tau inversion recovery (STIR) image reveals soft tissue metastasis in right side of pelvic cavity (arrow). (B) Coronal STIR image of the different patient reveals soft tissue metastasis in medial aspect of left upper thigh (arrow). (C) Coronal STIR image reveals two pulmonary nodules in right lower lung field (arrow).

Discussion

To the best of our knowledge, there has been no previous study that investigates the agreement of these two modalities in patients with HCC. The per-patient agreement between BS and WB-MRI with linear weighted *kappa* of 0.5 was considered moderate. WB-MRI tended to detect more lesions, with different detectability for different anatomical sites. This is not beyond the expectation, as the abilities to detect bone lesions by the two modalities are different. Lesions that do not present a sufficient osteoblastic reaction, such as small lesions or very aggressive lesions that causes rapid, intense destruction with little reactive bone formation will result in normal or low uptake of the radiotracer and will be difficult to detect by BS. The nature of frequent, pure osteolytic HCC metastatic bone lesions is one of the explanations for the false-negative results of BS. MRI, however, can detect such lesions very efficiently (Figure 1). Another characteristic MRI finding of bone metastases in HCC

is an intramedullary lesion with associated soft tissue mass, correlating with a previous study. [1] If the intramedullary lesion does not extend to the cortex, the lesion may not be detected by BS. These were shown in many spine and pelvic lesions in our study (Figure 1).

On the other hand, a lesion with sufficient osteoblastic reaction, even though small, is detected by BS. These were shown in our patients in whom WB-MRI could not detect five of 11 rib lesions (45%) that were well-shown in BS (Figure 2). These findings were also reported in a study of renal cancer patients. [4] It has been suggested that this limitation is due to artifact caused by pulsation and breathing motion in the thorax, which makes detection of lesions in ribs, sternum and scapula difficult. [4] Furthermore, flat bones are not well visualized on the coronal imaging and can be missed by MRI. Another limitation of the WB-MRI is artifact due to massive ascites; this caused one false negative in our patient.

Finally, although BS is generally accepted to be the standard tool in detection of bone metastasis, and uniform agreement of lesions categorization among different nuclear medicine physician has been reported [6]; the high sensitivity and low specificity nature of BS make it difficult to set its diagnostic criteria. This causes potential variations in BS interpretation, especially in circumstances of potentially normal or low radiotracer uptake lesions. This is also partially true for MRI, though MRI is more specific than BS; still it is not perfect.

Additional finding of extra-osseous lesions detected by WB-MRI (Figure 3) in 56% of cases in our study is within the range of that in previous studies. [4] This finding emphasizes another advantage of WB-MRI over BS, which is that it provides additional information and may lead to changes in patients' management. [7, 8]

In conclusion, there was only a moderate agreement in detection of HCC bone metastasis between BS and WB-MRI. Each modality had its own advantages and disadvantages. MRI tended to detect more lesions and was also useful for detection of extra-osseous lesions.

Acknowledgements

The authors would like to thank the technician teams of the nuclear medicine and MRI Units, the Department of Radiology, King Chulalongkorn Memorial Hospital. Also, the authors, hereby declare no conflict of interest in this study.

References

1. Kuhlman JE, Fishman EK, Leichner PK, Magid D, Order SE, Siegelman SS. Skeletal metastases from hepatoma: frequency, distribution, and radiographic features. Radiology 1986;160: 175-8.
2. Katyal S, Oliver JH 3rd, Peterson MS, Ferris JV, Carr BS, Baron RL. Extrahepatic metastases of hepatocellular carcinoma. Radiology 2000; 216:698-703.
3. Balliu E, Boada M, Pelaez I, Vilanova JC, Barcelo-Vidal C, Rubio A, et al. Comparative study of whole-body MRI and bone scintigraphy for the detection of bone metastases. Clin Radiol 2010;65:989-96
4. Sohaib SA, Cook G, Allen SD, Hughes M, Eisen T, Gore M. Comparison of whole-body MRI and bone scintigraphy in the detection of bone

metastases in renal cancer. Br J Radiol 2009;82:632-9.

5. Cascini G, Falcone C, Greco C, Bertucci B, Cipullo S, Tamburrini O. Whole-body magnetic resonance imaging for detecting bone metastases: comparison with bone scintigraphy. Radiol Med 2008;113:1157-70.
6. Zacho HD, Barsi T, Mortensen JC, Mogensen MK, Bertelsen H, Josephsen N,et al. Prospective multicenter study of bone scintigraphy in consecutive patients with newly diagnosed prostate cancer. Clin Nucl Med 2014;39: 26-31.
7. Walker R, Kessar P, Blanchard R, Dimasi M, Harper K, DeCarvalho V, et al. Turbo STIR magnetic resonance imaging as a whole-body screening tool for metastases in patients with breast carcinoma: preliminary clinical experience. J Magn Reson Imaging 2000;11: 343-50.
8. Eustace S, Tello R, DeCarvalho V, Carey J, Wroblicka JT, Melhem ER, et al. A comparison of whole-body turbo STIR MR imaging and planar 99mTc-methylene diphosphonate scintigraphy in the examination of patients with suspected skeletal metastases. AJR Am J Roentgenol 1997;169:1655-61.